

Properties of off-axis hollow Gaussian-Schell model vortex beam propagating in turbulent atmosphere

Yan-Song Song(宋延嵩), Ke-Yan Dong(董科研), Shuai Chang(常帅), Yan Dong(董岩), Lei Zhang(张雷)

Citation: Chin. Phys. B . 2020, 29(6): 064213 . **doi:** 10.1088/1674-1056/ab836c
Journal homepage: http://cpb.iphy.ac.cn; http://iopscience.iop.org/cpb

What follows is a list of articles you may be interested in

Paraxial propagation of cosh-Airy vortex beams in chiral medium

Xiao-Jin Yang(杨小锦), Zhen-Sen Wu(吴振森), Tan Qu(屈檀)

Chin. Phys. B . 2020, 29(3): 034201 . **doi:** 10.1088/1674-1056/ab683f

Comparison of three kinds of polarized Bessel vortex beams propagating through uniaxial anisotropic media

Jia-Wei Liu(刘佳伟), Hai-Ying Li(李海英), Wei Ding(丁炜), Lu Bai(白璐), Zhen-Sen Wu(吴振森), Zheng-Jun Li(李正军)

Chin. Phys. B . 2019, 28(9): 094214 . **doi:** 10.1088/1674-1056/ab37f5

Nonparaxial propagation properties of the chirped Airy Gaussian vortex beams in uniaxial crystals orthogonal to the optical axis

Yizuo Chen(陈奕佐), Guanwen Zhao(赵官文), Feng Ye(叶峰), Chuangjie Xu(许创杰), Dongmei Deng(邓冬梅)

Chin. Phys. B . 2018, 27(10): 104201 . **doi:** 10.1088/1674-1056/27/10/104201

Orbital angular momentum density and spiral spectra of Lorentz-Gauss vortex beams passing through a single slit

Zhi-Yue Ji(季志跃), Guo-Quan Zhou(周国泉)

Chin. Phys. B . 2017, 26(9): 094202 . **doi:** 10.1088/1674-1056/26/9/094202

Propagation of Airy Gaussian vortex beams in uniaxial crystals

Weihao Yu(余伟浩), Ruihuang Zhao(赵瑞璜), Fu Deng(邓富), Jiayao Huang(黄加耀), Chidao Chen(陈迟到), Xiangbo Yang(杨湘波), Yanping Zhao(赵燕平), Dongmei Deng(邓冬梅)

Chin. Phys. B . 2016, 25(4): 044201 . **doi:** 10.1088/1674-1056/25/4/044201

Properties of off-axis hollow Gaussian–Schell model vortex beam propagating in turbulent atmosphere*

Yan-Song Song(宋延嵩), Ke-Yan Dong(董科研)†, Shuai Chang(常帅), Yan Dong(董岩), and Lei Zhang(张雷)

National and Local Joint Engineering Research Center of Space Optoelectronics Technology, Changchun University of Science and Technology, Changchun 130022, *China*

(Received 26 August 2019; revised manuscript received 24 February 2020; accepted manuscript online 26 March 2020)

The analytical expression of off-axis hollow Gaussian–Schell model vortex beam (HGSMVB) generated by anisotropic Gaussian–Schell model source is first introduced. The evolution properties of off-axis HGSMVB propagating in turbulent atmosphere are analyzed. The results show that the off-axis HGSMVB with smaller coherence length or propagating in stronger turbulent atmosphere will evolve from dark hollow beam into Gaussian-like beam with a larger beam spot faster. The beams with different values of integer order N or the position for hollow and vortex factor R will have almost the same Gaussian-like spot distribution at the longer propagation distance.

Keywords: vortex beam, off-axis beam, Gaussian–Schell model sources, laser propagation, intensity

PACS: 42.68.Ay, 42.25.Bs **DOI:** 10.1088/1674-1056/ab836c

1. Introduction

The propagation properties of various laser beams in a turbulent medium have been widely investigated in past years, and the evolution properties will affect the applications of laser beams in wireless optical communication and sensing. The influences of turbulent medium on propagation properties of coherent laser beams and partially coherent laser beams are both studied. For examples, Cai *et al.* have reviewed the properties of partially coherent beams in turbulent atmosphere.[1] Until now, the propagation properties of many partially coherent beams in a turbulent medium have been studied, such as partially coherent electromagnetic beams,[2,3] off-axis Gaussian–Schell model beam and partially coherent laser array beam,[4] apertured partially coherent beam,[5] partially coherent rectangular flat-topped laser array,[6] partially coherent Lorentz–Gauss beam,[7] partially coherent elegant Hermite–Gaussian beam,[8] partially coherent Laguerre–Gaussian beam,[9] phase-locked partially coherent flat topped laser beam array,[10] radial phased-locked partially coherent anomalous hollow beam array,[11] Laguerre–Gaussian correlated Schell-model beam,[12] partially coherent four-petal Gaussian vortex beam,[13] radial phased-locked partially coherent flat-topped vortex beam array,[14] multi-cosine-Laguerre–Gaussian correlated Schell-model beam,[15] partially coherent Lorentz–Gauss vortex beam,[16] partially coherent anomalous elliptical hollow Gaussian beam,[17] partially coherent flat-topped vortex hollow beam,[18] partially coherent crescent-like optical beam,[19] partially coherent Lorentz–Gauss beam,[20] radial phased-locked partially coherent Lorentz–Gauss array beam,[21] truncated Gaussian–Schell model beam,[22] partially coherent anomalous hollow vortex beam,[23] partially coherent elegant Hermite–Cosh–Gaussiands beam,[24] Hankel–Bessel beams,[25] Laguerre–Gaussian beams,[26] multi-Gaussian–Schell model beams carrying an edge dislocation,[27] and rectangular multi-Gaussian–Schell model array beam.[28] On the other hand, the studies of off-axis beam have attracted much attention.[29–31] Recently, a new beam called off-axis hollow vortex Gaussian beam has been introduced in theory.[32] From previous report,[1] it can been found that the partially coherent beams have advantage over fully coherent beams in mitigating the effect of atmospheric turbulence. Hence, it is very interesting to investigate what will happen when the spatial coherence length is introduced into the off-axis hollow vortex Gaussian beam. In this paper, a beam called off-axis hollow Gaussian–Schell model vortex beam (HGSMVB) generated by the Gaussian–Schell model source is first introduced. Then, the cross-spectral density of off-axis HGSMVB propagating in turbulent atmosphere is derived. Finally, the influences of beam parameter and turbulent atmosphere on the intensity and coherence properties of off-axis HGSMVB are illustrated and analyzed by using numerical examples.

2. Theoretical model

From previous work, the analytical expression of off-axis hollow vortex beam at the plane $z = 0$ can be described by[32]

$$E(\boldsymbol{r}_0, 0) = C_0 \left[(x_0 - R_x)^2 + (y_0 - R_y)^2 \right]^N$$

*Project supported by the Natural Science Foundation of Jilin Province, China (Grant No. 20180101031JC) and the Jilin Provincial Science Foundation for Basic Research, China (Grant No. 2019C040-7).

†Corresponding author. E-mail: dongkeyan2018@sohu.com

© 2020 Chinese Physical Society and IOP Publishing Ltd

$$\times \left[(x_0 - R_x) + \mathrm{i}\,(y_0 - R_y)\right]^M \exp\left(-\frac{x_0^2 + y_0^2}{w_0^2}\right), \quad (1)$$

where $\boldsymbol{r}_0 = (x_0, y_0)$ is the position vector at the plane $z = 0$, w_0 is the width of Gaussian beam, (R_x, R_y) is the position of hollow and vortex factor, N is an integer order, M is the topological charge, C_0 is a constant.

Consider the method of generating the partially coherent beams, then the cross-spectral density (CSD) of off-axis hollow Gaussian–Schell model vortex beam (HGSMVB) generated by anisotropic Gaussian–Schell model sources will be expressed as[33]

$$\begin{aligned}
&\Gamma(\boldsymbol{r}_{10}, \boldsymbol{r}_{20}, 0) \\
&= C_0 \left[(x_{10} - R_x)^2 + (y_{10} - R_y)^2\right]^N \\
&\quad \times \left[(x_{10} - R_x) + \mathrm{i}\,(y_{10} - R_y)\right]^M \exp\left(-\frac{x_{10}^2 + y_{10}^2}{w_0^2}\right) \\
&\quad \times C_0 \left[(x_{20} - R_x)^2 + (y_{20} - R_y)^2\right]^N \\
&\quad \times \left[(x_{20} - R_x) - \mathrm{i}\,(y_{20} - R_y)\right]^M \exp\left(-\frac{x_{20}^2 + y_{20}^2}{w_0^2}\right) \\
&\quad \times \exp\left[-\frac{(x_{10} - x_{20})^2}{2\sigma_x^2} - \frac{(y_{10} - y_{20})^2}{2\sigma_y^2}\right], \quad (2)
\end{aligned}$$

where σ_x and σ_y are the coherence length in the x- and y-axis directions, respectively.

Under the paraxial approximation, the CSD of off-axis HGSMVB propagating in turbulent atmosphere at the plane z can be written by the extended Huygens–Fresnel integral as follows:[1–7]

$$\begin{aligned}
&\Gamma(\boldsymbol{r}_1, \boldsymbol{r}_2, z) \\
&= \frac{k^2}{4\pi^2 z^2} \int_{-\infty}^{+\infty}\int_{-\infty}^{+\infty}\int_{-\infty}^{+\infty}\int_{-\infty}^{+\infty} \Gamma(\boldsymbol{r}_{10}, \boldsymbol{r}_{20}, 0) \\
&\quad \times \exp\left[-\frac{\mathrm{i}k}{2z}(\boldsymbol{r}_1 - \mathbf{r}_{10})^2 + \frac{\mathrm{i}k}{2z}(\boldsymbol{r}_2 - \mathbf{r}_{20})^2\right] \\
&\quad \times \langle \exp\left[\psi(\boldsymbol{r}_{10}, \boldsymbol{r}_1) + \psi^*(\boldsymbol{r}_{20}, \boldsymbol{r}_2)\right]\rangle \,\mathrm{d}\boldsymbol{r}_{10}\,\mathrm{d}\boldsymbol{r}_{20} \quad (3)
\end{aligned}$$

with

$$\begin{aligned}
&\langle \exp\left[\psi(\boldsymbol{r}_{10}, \boldsymbol{r}_1) + \psi^*(\boldsymbol{r}_{20}, \boldsymbol{r}_2)\right]\rangle \\
&= \exp\left[-\frac{(\boldsymbol{r}_{10} - \boldsymbol{r}_{20})^2 + (\boldsymbol{r}_{10} - \boldsymbol{r}_{20})(\boldsymbol{r}_1 - \boldsymbol{r}_2) + (\boldsymbol{r}_1 - \boldsymbol{r}_2)^2}{\rho_0^2}\right], \quad (4)
\end{aligned}$$

$$\rho_0 = \left(0.545 C_n^2 k^2 z\right)^{-3/5}, \quad (5)$$

where C_n^2 is the constant of refractive index structure for turbulent atmosphere; $k = 2\pi/\lambda$ is the wave number, and λ is the wavelength.

Substituting Eq. (2) into Eq. (3), and considering the following equations:

$$(x + y)^M = \sum_{l=0}^{M} \frac{M!}{l!\,(M - l)!} x^{M-l} y^l, \quad (6)$$

$$\begin{aligned}
&\int_{-\infty}^{+\infty} x^n \exp\left(-px^2 + 2qx\right) \mathrm{d}x \\
&= n! \exp\left(\frac{q^2}{p}\right)\left(\frac{q}{p}\right)^n \sqrt{\frac{\pi}{p}} \sum_{k=0}^{[n/2]} \frac{1}{k!\,(n - 2k)!}\left(\frac{p}{4q^2}\right)^k, \quad (7)
\end{aligned}$$

$$H_n(x) = \sum_{l=0}^{[n/2]} \frac{(-1)^l n!}{l!\,(n - 2l)!} (2x)^{n-2l}, \quad (8)$$

the CSD of off-axis HGSMVB propagating in turbulent atmosphere can be derived as

$$\begin{aligned}
&\Gamma(\boldsymbol{r}_1, \boldsymbol{r}_2, z) \\
&= \frac{k^2}{4\pi^2 z^2} \exp\left[-\frac{\mathrm{i}k}{2z}\left(x_1^2 + y_1^2\right) + \frac{\mathrm{i}k}{2z}\left(x_2^2 + y_2^2\right)\right] \\
&\quad \times \exp\left[-\frac{(x_1 - x_2)^2 + (y_1 - y_2)^2}{\rho_0^2}\right] \\
&\quad \times C_0 \exp\left(-\frac{R_x^2}{w_0^2} - \frac{R_y^2}{w_0^2}\right) \sum_{n=0}^{N} \frac{N!}{n!\,(N - n)!} \sum_{m=0}^{M} \frac{M!\, i^m}{m!\,(M - m)!} \\
&\quad \times C_0 \exp\left(-\frac{R_x^2}{w_0^2} - \frac{R_y^2}{w_0^2}\right) \sum_{s=0}^{N} \frac{N!}{s!\,(N - s)!} \sum_{t=0}^{M} \frac{M!\,(-i)^t}{t!\,(M - t)!} \\
&\quad \exp\left[-\frac{\mathrm{i}k}{2z}\left(2x_2 R_x - 2x_1 R_x\right)\right] \exp\left[-\frac{\mathrm{i}k}{2z}\left(2y_2 R_y - 2y_1 R_y\right)\right] \\
&\quad \times \Gamma(x, z)\,\Gamma(y, z), \quad (9)
\end{aligned}$$

where

$$\begin{aligned}
\Gamma(x, z) &= \sqrt{\frac{\pi}{a_x}}\,(2(N - n) + M - m)! \exp\left[\frac{1}{a_x}\left[\frac{\mathrm{i}k}{2z}(x_1 - R_x) - \frac{R_x}{w_0^2} - \frac{x_1 - x_2}{2\rho_0^2}\right]^2\right] \\
&\quad \times \left(\frac{1}{a_x}\right)^{2(N-n)+M-m} \sum_{d=0}^{\left[\frac{2(N-n)+M-m}{2}\right]} \frac{1}{d!\,(2(N - n) + M - m - 2d)!} \left(\frac{a_x}{4}\right)^d \sum_{l=0}^{2(N-n)+M-m-2d} \frac{[2(N - n) + M - m - 2d]!}{l!\,(2(N - n) + M - m - 2d - l)!} \\
&\quad \times \left[\frac{\mathrm{i}k}{2z}(x_1 - R_x) - \frac{R_x}{w_0^2} - \frac{x_1 - x_2}{2\rho_0^2}\right]^{2(N-n)+M-m-2d-l} \left(\frac{1}{2\sigma_x^2} + \frac{1}{\rho_0^2}\right)^l \sqrt{\frac{\pi}{b_x}}\, 2^{-(2(N-s)+M-t+l)}\, \mathrm{i}^{2(N-s)+M-t+l} \\
&\quad \times \exp\left(\frac{c_x^2}{b_x}\right)\left(\frac{1}{b_x}\right)^{0.5(2(N-s)+M-t+l)} H_{2(N-s)+M-t+l}\left(-\frac{\mathrm{i}c_x}{\sqrt{b_x}}\right) \quad (10)
\end{aligned}$$

with

$$a_x = \frac{1}{w_0^2}+\frac{1}{2\sigma_x^2}+\frac{1}{\rho_0^2}+\frac{\mathrm{i}k}{2z}, \tag{11}$$

$$b_x = \frac{1}{w_0^2}+\frac{1}{2\sigma_x^2}+\frac{1}{\rho_0^2}-\frac{\mathrm{i}k}{2z}-\frac{1}{a_x}\left(\frac{1}{2\sigma_x^2}+\frac{1}{\rho_0^2}\right)^2, \tag{12}$$

$$\begin{aligned} c_x = {} & \frac{\mathrm{i}k}{2z}(R_x-x_2)-\frac{R_x}{w_0^2}+\frac{x_1-x_2}{2\rho_0^2} \\ & +\frac{1}{a_x}\left[\frac{\mathrm{i}k}{2z}(x_1-R_x)-\frac{R_x}{w_0^2}-\frac{x_1-x_2}{2\rho_0^2}\right] \\ & \times\left(\frac{1}{2\sigma_x^2}+\frac{1}{\rho_0^2}\right), \end{aligned} \tag{13}$$

$$\begin{aligned} & \Gamma(y,z) \\ = {} & \sqrt{\frac{\pi}{a_y}}(2n+m)!\exp\left[\frac{1}{a_y}\left[\frac{\mathrm{i}k}{2z}(y_1-R_y)-\frac{R_y}{w_0^2}-\frac{y_1-y_2}{2\rho_0^2}\right]^2\right] \\ & \times\left(\frac{1}{a_y}\right)^{2n+m}\sum_{d=0}^{[(2n+m)/2]}\frac{1}{d!(2n+m-2d)!}\left(\frac{a_y}{4}\right)^d \\ & \times\sum_{l=0}^{2n+m-2d}\frac{(2n+m-2d)!}{l!(2n+m-2d-l)!} \\ & \times\left[\frac{\mathrm{i}k}{2z}(y_1-R_y)-\frac{R_y}{w_0^2}-\frac{y_1-y_2}{2\rho_0^2}\right]^{2n+m-2d-l} \\ & \times\left(\frac{1}{2\sigma_y^2}+\frac{1}{\rho_0^2}\right)^l\sqrt{\frac{\pi}{b_y}}2^{-(2s+t+l)}\mathrm{i}^{2s+t+l} \\ & \times\exp\left(\frac{c_y^2}{b_y}\right)\left(\frac{1}{b_y}\right)^{0.5(2s+t+l)}H_{2s+t+l}\left(-\frac{\mathrm{i}c_y}{\sqrt{b_y}}\right) \end{aligned} \tag{14}$$

with

$$a_y = \frac{1}{w_0^2}+\frac{1}{2\sigma_y^2}+\frac{1}{\rho_0^2}+\frac{\mathrm{i}k}{2z}, \tag{15}$$

$$b_y = \frac{1}{w_0^2}+\frac{1}{2\sigma_y^2}+\frac{1}{\rho_0^2}-\frac{\mathrm{i}k}{2z}-\frac{1}{a_y}\left(\frac{1}{2\sigma_y^2}+\frac{1}{\rho_0^2}\right)^2, \tag{16}$$

$$\begin{aligned} c_y = {} & \frac{\mathrm{i}k}{2z}(R_y-y_2)-\frac{R_y}{w_0^2}+\frac{y_1-y_2}{2\rho_0^2} \\ & +\frac{1}{a_y}\left[\frac{\mathrm{i}k}{2z}(y_1-R_y)-\frac{R_y}{w_0^2}-\frac{y_1-y_2}{2\rho_0^2}\right] \\ & \times\left(\frac{1}{2\sigma_y^2}+\frac{1}{\rho_0^2}\right). \end{aligned} \tag{17}$$

The average intensity of off-axis HGSMVB propagating in turbulent atmosphere can be obtained by[33]

$$I(\boldsymbol{r},z)=\Gamma(\boldsymbol{r},\boldsymbol{r},z). \tag{18}$$

The spectral degree of coherence for off-axis HGSMVB propagating in turbulent atmosphere at the different points $\boldsymbol{r}_1=(x_1,y_1)$ and $\boldsymbol{r}_2=(x_2,y_2)$ can be described by[34]

$$\mu(\boldsymbol{r}_1,\boldsymbol{r}_2,z)=\frac{\Gamma(\boldsymbol{r}_1,\boldsymbol{r}_2,z)}{[\Gamma(\boldsymbol{r}_1,\boldsymbol{r}_1,z)\Gamma(\boldsymbol{r}_2,\boldsymbol{r}_2,z)]^{1/2}}. \tag{19}$$

3. Analyses and discussion

The average intensity and spectral degree of coherence of off-axis HGSMVB propagating in turbulent atmosphere are illustrated and analyzed in this section. In the numerical analyses, the parameters are set to be $w_0=1$ cm, $N=2$, $M=1$, $R_x=1$ mm, $R_y=0$, $\lambda=800$ nm, and $C_n^2=10^{-14}$ m$^{-2/3}$.

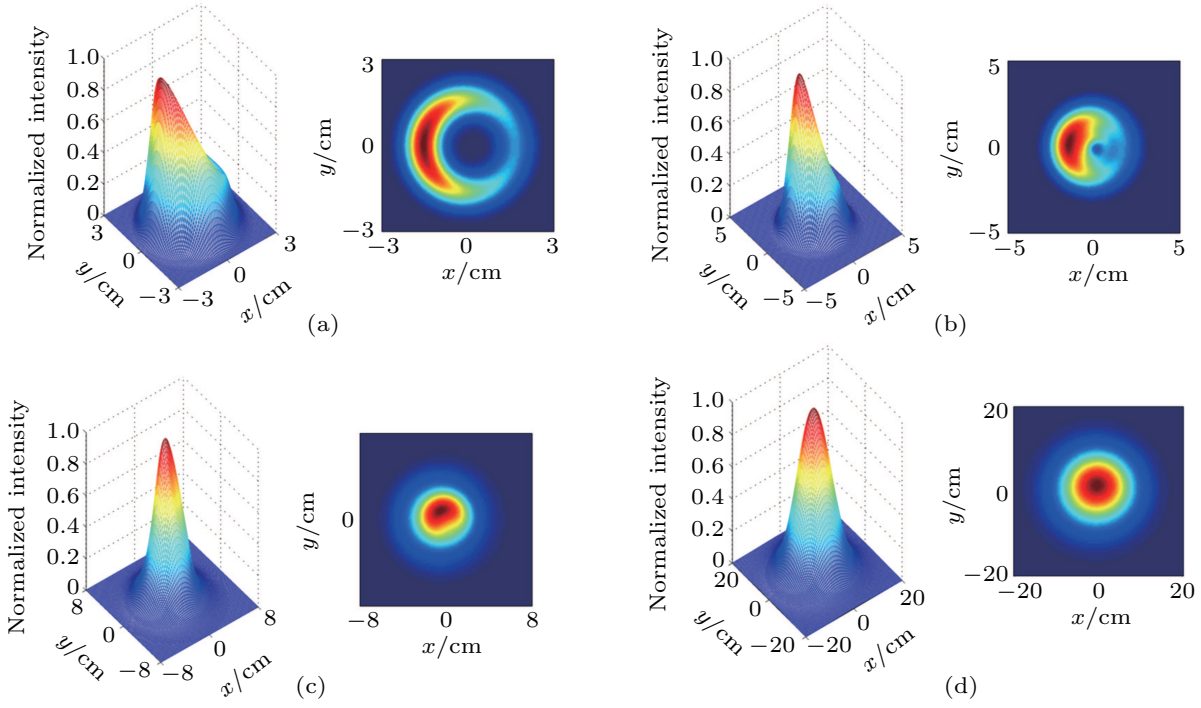


Fig. 1. Intensity and contour graphs of off-axis HGSMVB propagating in turbulent atmosphere for $z=100$ m (a), 300 m (b), 1000 m (c), and 3000 m (d).

To investigate the average intensity properties of off-axis HGSMVB propagating in different media, the intensity of off-axis HGSMVB with $\sigma_x = \sigma_y = 2$ cm propagating in turbulent atmosphere and free space are illustrated in Figs. 1 and 2, respectively. We can see that the dark hollow center of off-axis HGSMVB in turbulent atmosphere gradually disappears and the average intensity in the center increases as the propagation distance z increases (Figs. 1(a) and 1(b)); when the propagation distance increases to a longer distance $z = 3000$ m, the off-axis HGSMVB in turbulent atmosphere evolves into a Gaussian-like beam (Fig. 1(d)). While the off-axis HGSMVB propagating in free space also gradually loses the dark hollow center as the propagation distance z increases, but average intensity distribution of the off-axis HGSMVB in free space at the propagation distance $z = 3000$ m does not evolve into that of the Gaussian beam. Thus, the turbulent atmosphere will accelerate the evolution of off-axis HGSMVB into the Gaussian-like beam. The reason why the off-axis HGSMVB in turbulent atmosphere evolves into the Gaussian-like beam at the longer propagation distance is that the general beam propagating in turbulent atmosphere evolves into Gaussian-like beam.[1,35]

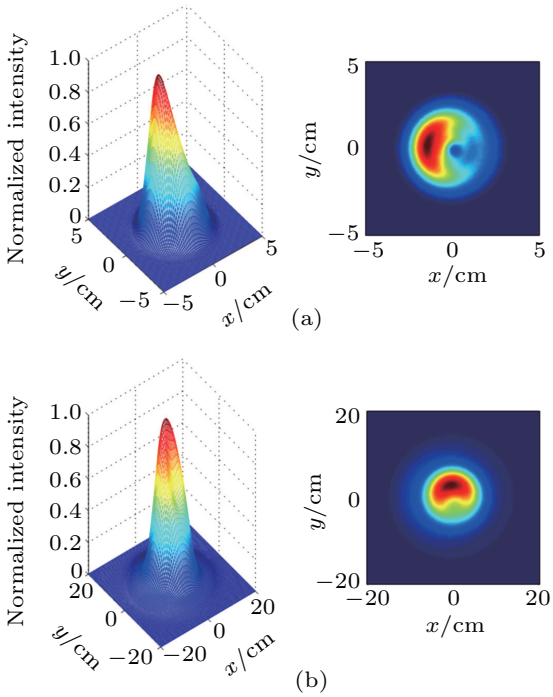


Fig. 2. Intensity and contour graphs of off-axis HGSMVB propagating in free spac for $z = 300$ m (a) and 3000 m (b).

To investigate the effects of strength of turbulent atmosphere on evolution properties, the cross sections of off-axis HGSMVB propagation in the different turbulent atmospheres are illustrated in Fig. 3. One can see that the off-axis HGSMVB propagating in free space ($C_n^2 = 0$) evolves into the Gaussian-like beam slower than the off-axis HGSMVB propagating in turbulent atmosphere, and the off-axis HGSMVB propagating in stronger turbulent atmosphere loses the dark hollow center faster, and the off-axis HGSMVB propagating in stronger turbulent atmosphere has a larger beam spot for the same propagation distance (Fig. 3(b)).

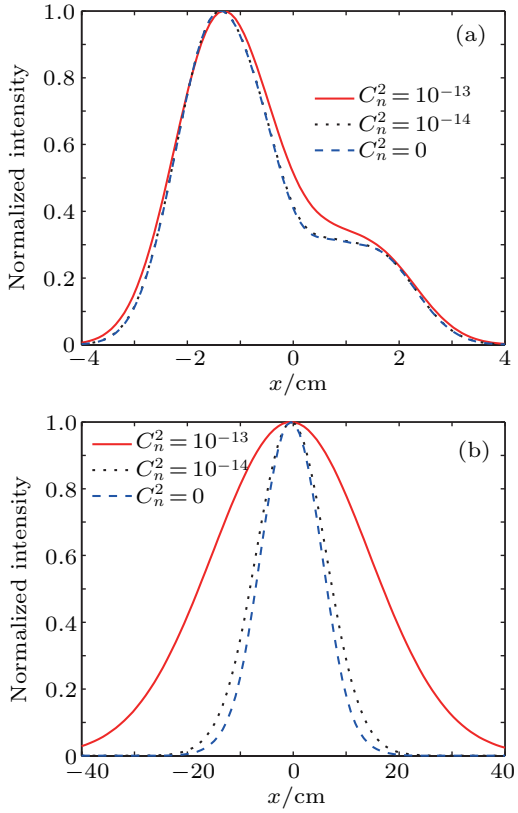


Fig. 3. Cross sections of off-axis HGSMVB propagating in turbulent atmosphere for different values of C_n^2 and $z = 400$ m (a) and 3000 m (b).

To investigate the effects of different values of beam parameters $\sigma_x = \sigma_y = \sigma$, N, M, and $R = R_x$ on the spreading properties of off-axis HGSMVB, the cross sections of off-axis HGSMVB propagating in turbulent atmosphere for the different values of parameters σ, N, M, and R are shown in Figs. 4–7, respectively. In Fig. 4, it is shown that the off-axis HGSMVB with smaller coherence length σ will lose the dark hollow center and evolve into a beam with intensity in the center faster (Fig. 4(a)); as the propagation distance z increases to a larger distance $z = 2000$ m, the off-axis HGSMVBs with different values of coherence length σ can all evolve into the Gaussian-like beams, but the off-axis HGSMVB with larger coherence length σ has a smaller beam spot. The off-axis HGSMVB with smaller order N has a smaller hollow center (Fig. 5(a)), and the influence of order N on the intensity of off-axis HGSMVB will disappear at the longer propagation distance (Fig. 5(b)). The off-axis HGSMVB with smaller topological charge M propagating in turbulent atmosphere evolves into Gaussian-like beam faster, but which will have a smaller beam spot when the off-axis HGSMVBs with the different values of M all evolve into the Gaussian-like beams (Fig. 6(b)). As the R increases, the circular symmetry of

off-axis HGSMVB is destroyed, and the influence of R on the far field distribution of average intensity of off-axis HGSMVB disappears as the off-axis HGSMVBs all evolve from dark hollow center beam into the Gaussian-like beam (Fig. 7(b)).

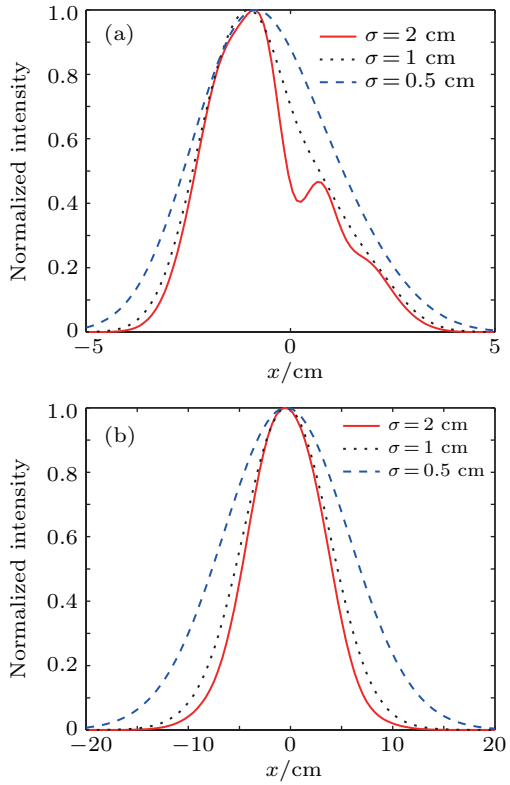


Fig. 4. Cross sections of off-axis HGSMVB propagating in turbulent atmosphere for different values of $\sigma_x = \sigma_y$ and $z = 400$ m (a) and 2000 m (b).

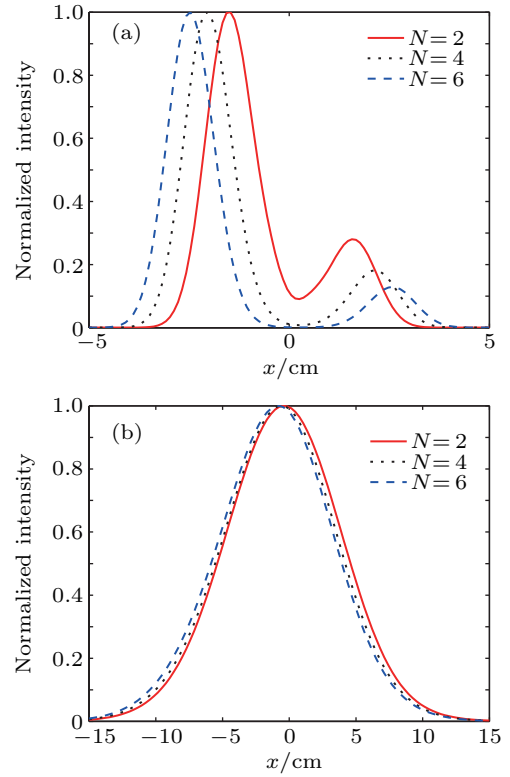


Fig. 5. Cross sections of off-axis HGSMVB propagating in turbulent atmosphere for different values of N and $z = 400$ m (a) and 2000 m (b).

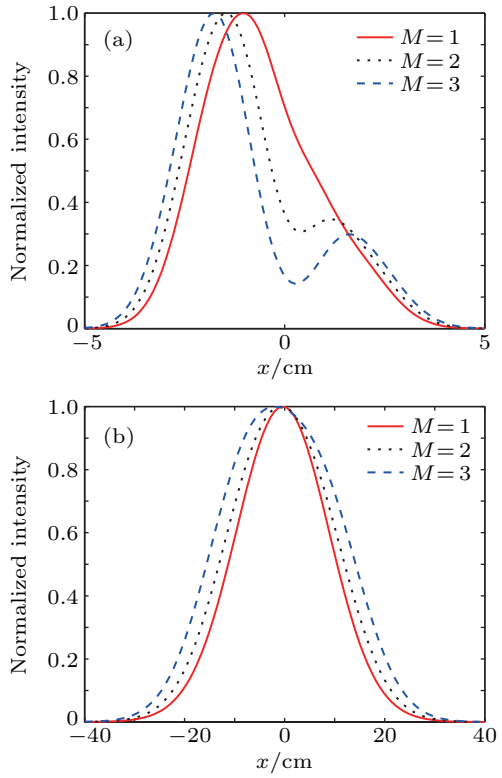


Fig. 6. Cross sections of off-axis HGSMVB propagating in turbulent atmosphere for different values of M and $z = 400$ m (a) and 4000 m (b).

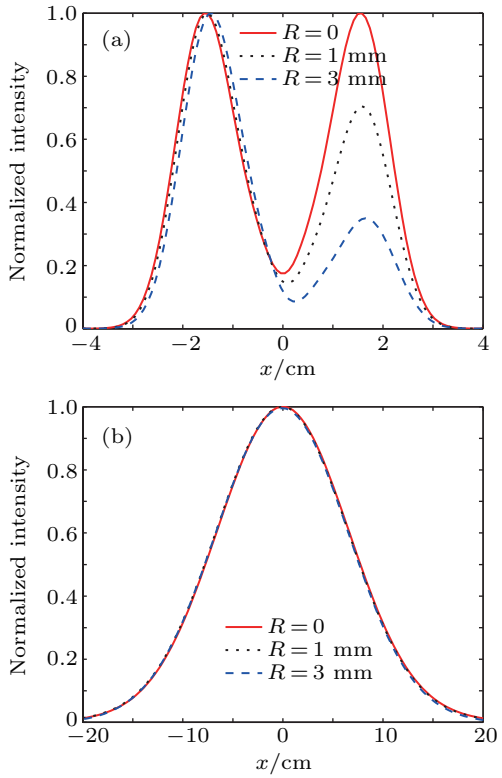


Fig. 7. Cross sections of off-axis HGSMVB propagating in turbulent atmosphere for different values of $R = R_x$ and $z = 200$ m (a) and 3000 m (b).

The spectral degrees of coherence of off-axis HGSMVB propagating in turbulent atmosphere for the different values of parameters M, N, σ, and R are illustrated in Figs. 8 and 9, the two points are set to be $(x,0)$ and $(0,0)$. As can be

seen from Fig. 8, the spectral degree of coherence of off-axis HGSMVB propagating in turbulent atmosphere for the different values of M decreases as the distance between the two points $(x,0)$ and $(0,0)$ increases to the longer propagation distance $z = 3000$ m. The influences of beam parameters M, N, σ, and R on the spectral degrees of coherence of off-axis HGSMVB propagating in turbulent atmosphere at the longer propagation distance $z = 3000$ m are given in Fig. 9. One can see that the influences of the different values of parameters M, N, σ, and R on the spectral degree of coherence disappear as the distance between two points $(x,0)$ and $(0,0)$ increases to a certain distance. When the distance between two points $(x,0)$ and $(0,0)$ is smaller, the spectral degrees of coherence of off-axis HGSMVB with larger values of M, N or R decrease more rapidly than the off-axis HGSMVB with smaller values of M, N or R. While, the spectral degree of coherence of off-axis HGSMVB is not affected by the coherence length σ at the longer propagation distance $z = 3000$ m.

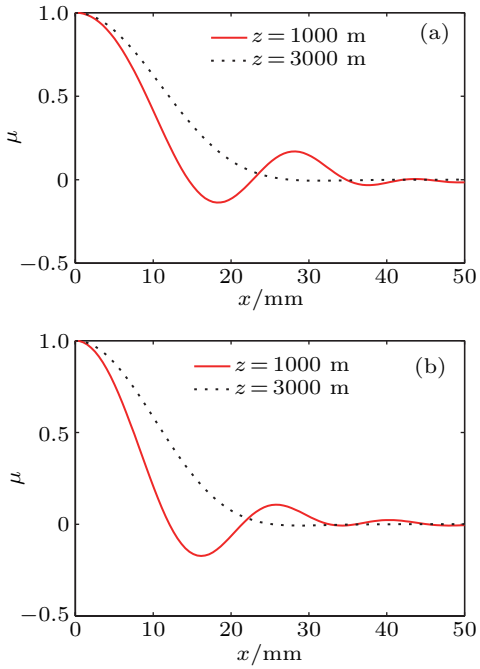


Fig. 8. Spectral degrees of coherence of off-axis HGSMVB propagating in turbulent atmosphere for different values of distance z and $M = 1$ (a) and 3 (b).

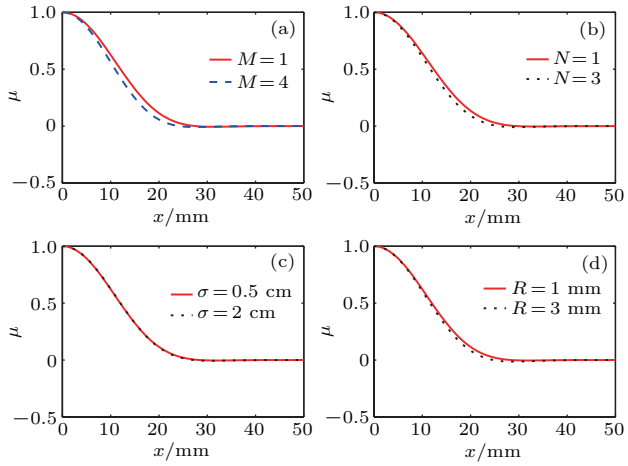


Fig. 9. Spectral degrees of coherence of off-axis HGSMVB propagating in turbulent atmosphere at propagation distance $z = 3000$ m for different values of parameters M, N, σ, and R.

4. Conclusions

In this paper, the off-axis HGSMVB generated by anisotropic Gaussian–Schell model source is defined by using analytical expressions. The CSD of off-axis HGSMVB propagating in turbulent atmosphere is derived. The evolution properties of average intensity and spectral degree of coherence are illustrated and discussed. As the propagation distance z increases, the off-axis HGSMVB propagating in turbulent atmosphere evolves from dark hollow beam into the Gaussian-like beam due to the effects of turbulent atmosphere and coherence length σ. The off-axis HGSMVB with smaller coherence length σ or the off-axis HGSMVB propagating in stronger turbulent atmosphere (larger C_n^2) evolves from dark hollow beam into the Gaussian-like beam with a larger beam spot more rapidly. The influences of parameters N and R on the distribution of average intensity gradually disappears as the beam evolves into the Gaussian-like beam. The obtained results also show that the spectral degrees of coherence for the different points $(x,0)$ and $(0,0)$ decrease with the distance between two points at the longer propagation distance, and the spectral degrees of coherence of off-axis HGSMVB with larger M, N or R decrease more rapidly than the off-axis HGSMVB with smaller M, N or R. The research results may be useful in the real optical communication and remote sensing in turbulent atmosphere.

References

[1] Wang F, Liu X L and Cai Y J 2015 *Prog. Electromagn. Res.* **150** 123
[2] Salem M, Korotkova O, Dogariu A and Wolf E 2004 *Waves Random Media* **14** 513
[3] Roychowdhury H, Ponomarenko S A and Wolf E 2005 *J. Mod. Opt.* **52** 1611
[4] Cai Y J, Lin Q, Baykal Y and Eyyuboglu H T 2007 *Opt. Commun.* **278** 157
[5] Ji X and Ji G 2008 *Appl. Phys. B* **92** 111
[6] Zhou P, Ma Y X, Wang X L, Ma H T, Xu X J and Liu Z J 2009 *Appl. Opt.* **48** 5251
[7] Zhou G and Chu X 2010 *Appl. Phys. B* **100** 909
[8] Wang F, Cai Y, Eyyuboglu H T and Baykal Y 2011 *Appl. Phys. B* **103** 461
[9] Wang D, Wang F, Cai Y and Chen J 2012 *J. Mod. Opt.* **59** 372
[10] Razzaghi D, Hajiesmaeilbaigi F and Alavinejad M 2013 *Optik* **124** 2135
[11] Wang K L and Zhao C H 2014 *Opt. Laser Technol.* **57** 44
[12] Zhu Z R, Liu L, Wang F and Cai Y J 2015 *J. Opt. Soc. Am. A* **32** 374
[13] Liu D J, Wang Y C and Yin H M 2016 *Opt. Laser Technol.* **78** 95
[14] Liu H L, Lu Y F, Xia J, Chen D, He W and Pu X Y 2016 *Opt. Express* **24** 19695
[15] Zhu J, Li X, Tang H and Zhu K 2017 *Opt. Express* **25** 20071
[16] Liu D, Yin H, Wang G and Wang Y 2017 *Appl. Opt.* **56** 8785
[17] Tian H H, Xu Y G, Yang T, Ma Z R, Wang S J and Dan Y Q 2017 *J. Mod. Opt.* **64** 422
[18] Liu D J, Luo X X, Yin H M, Wang G Q and Wang Y C 2017 *Optik* **130** 227

[19] Wang F, Li J, Martinez-Piedra G and Korotkova O 2017 *Opt. Express* **25** 26055
[20] Liu D, Wang G and Wang Y 2018 *Opt. Laser Technol.* **98** 309
[21] Liu D and Wang Y 2018 *Opt. Laser Technol.* **103** 33
[22] Hu Y, Dong X, Zhao N, Zhao X and Xu S 2019 *Opt. Commun.* **436** 82
[23] Liu D, Wang G, Yin H, Zhong H and Wang Y 2019 *Opt. Commun.* **437** 346
[24] Zhang W F, Lian J, Wang Y S, Hu X Y, Sun M L, Zhao M L, Wang Y and Li M M 2015 *Chin. Phys. Lett.* **32** 64204
[25] Yin X L, Guo Y L, Yan H, Cui X Z, Chang H, Tian Q H, Wu G H, Zhang Q, Liu B and Xin X J 2018 *Acta Phys. Sin.* **67** 114201 (in Chinese)
[26] Cui X Z, Yin X L, Chang H, Zhang Z C, Wang Y J and Wu G H 2017 *Chin. Phys. B* **26** 114207
[27] Liu D J, Wang Y C, Wang G Q, Yin H M and Zhong H Y 2019 *Chin. Phys. B* **28** 104207
[28] Ma X L, Liu D J, Wang Y C, Yin H M, Zhong H Y and Wang G Q 2020 *Appl. Sci.* **10** 450
[29] Zheng C W 2006 *J. Opt. Soc. Am. A* **23** 2161
[30] Wang K L and Zhao C L 2015 *Opt. Commun.* **334** 280
[31] Li L, Huan Y Z, Wang Y C, Hua D, Yang X, Liu D J and Wang Y C 2019 *Optik* **194** 163133
[32] Chen G, Huang X, Xu C, Huang L, Xie J and Deng D 2019 *Opt. Express* **27** 6357
[33] Li Y and Wolf E 1982 *Opt. Lett.* **7** 256
[34] Wolf E 2003 *Phys. Lett. A* **312** 263
[35] Eyyuboglu H T, Baykal Y and Sermutlu E 2006 *Opt. Commun.* **265** 399